Modelling of Propellant Management Systems in Early-Phase Launcher Development

V. Clark[⋆†]
[⋆]*German Aerospace Center (DLR), Institute of Space Systems*
Bremen, Germany, vanessa.clark@dlr.de
[†]Corresponding author

Abstract

Liquid propellant storage, feed and management systems are an important domain in preliminary launcher design activities, as they drive system-level masses and vehicle layout. The Propellant Management Program (PMP) was developed by the German Aerospace Centre (DLR) department of Space Launcher Systems Analysis (SART) for rapid tank, feedline, pressurisation, cross-feeding and venting analysis. This program is an important part of DLR-SART's development toolbox, and has an intended application in the initial sizing of propellant storage and management systems for new launcher concepts. While the physical models behind the program, such as thermal behaviour of propellant and tanks in flight, are well-developed, the application of the program as a preliminary design tool is yet to be validated. A wealth of data is publicly available for the Saturn-V rocket, including stage fact sheets flight data from the Apollo missions. This paper details the simulation of the Saturn-V rocket propellant storage, feed and pressurisation systems, undertaken as part of the validation of PMP as a preliminary design tool. The high complexity of the layout and propellant management strategy of the Saturn-V rocket also provided additional functional requirements for future versions of PMP, and highlighted the need for a new pressurisation system control scheme.

Acronyms

CECO	Centre Engine Cut-Off
DLR	German Aerospace Centre
EDT	Eastern Daylight Time
FD	Fill and Drain
GH_2	Gaseous Hydrogen
GHe	Gaseous Helium
GO_2	Gaseous Oxygen
IR	Infrared
IU	Instrument Unit
LEO	Low Earth Orbit
LES	Launch Escape System
LH_2	Liquid Hydrogen
LO_2	Liquid Oxygen
NASA	National Aeronautics and Space Administration
NPSP	Net Positive Suction Pressure
OECO	Outer Engine Cut-Off
PMP	Propellant Management Program
RP-1	Kerosene
SART	Space Launcher Systems Analysis
S-IC	Saturn-V First Stage
S-II	Saturn-V Second Stage
S-IVB	Saturn-V Third Stage
TOSCA	Trajectory Optimisation and Simulation of Conventional and Advanced Space Transportation Systems
TLI	Trans-Lunar Injection

1. Introduction

In the current commercial launch vehicle industry, great effort is being expended to reduce the cost of access to space and increase the payload mass capacity of launchers. The high specific impulse of cryogenic propulsion systems make them ideal for addressing the latter of these.[1] Consequently, the design of light-weight cryogenic launch vehicle concepts and stages is a key task of the German Aerospace Centre (DLR) department of Space Launcher Systems Analysis (SART).

The propellant tanks are major components of cryogenic stages, and typically have an integral structural role as well as functional capacity. Thus, they are an important domain that drives system-level mass and vehicle layout in launch vehicle preliminary design. The influence of a cryogenic tank size and mass on the overall design is no more apparent than in the doomed X-33 project, where the failed test (solvable by a 500 kg increase in mass) of the composite Liquid Hydrogen (LH_2) tank led to the termination of the entire project.[2] Furthermore, the propellant management system, which encompasses the propellant feed system, venting, fill and drain lines, and the pressurisation system, also has a significant mass and should therefore be the subject of optimisation in early-phase design activities.[3]

At DLR-SART the in-house tool Propellant Management Program (PMP) was developed to perform rapid propellant tank and propellant management system sizing. The latter of these is particularly complex to analyse, and the use of empirical models is often insufficient due to the sensitivity of the system. Cryogenic stages involve the storage of liquid propellants at very low temperatures, resulting in complex fluid-mechanical and thermodynamic processes which have an impact on the pressurisation system design and need to be identified and controlled early in the stage design process. The gas pressure in the ullage of the propellant tanks has to be maintained within a pre-determined set of bounds that may themselves be transient as they are dictated by not only the structural stability requirements of the tanks but also the Net Positive Suction Pressure (NPSP) requirements of the engines' turbopumps. Ullage pressure decreases as the propellant is drained from the tanks, but is also influenced by propellant boil-off and thus by the thermal environment and loads on the stage. Tank pressurisation requires the use of on-board fluids, which can be either the gaseous form of the propellant or a non-reactive pressurant gas, such as Helium. This system and its regulation becomes even more complex when engine reignition is performed, or when the stage is subject to a long coasting phase on orbit.[1,4] The design and optimisation of the pressurisation system must therefore involve the simulation of the entire mission, including stage loads, manoeuvres, thermal loads, engine operation (including transients) and the logical control of the ullage pressures, including both pressurant gas injection and venting.

The physics models behind these phenomenon have been successfully implemented in PMP,[1] which is now being utilised for the preliminary design of propellant storage and feed systems for space transportation concepts including conventional launch vehicles, as outlined in *ref. 5*, and also advanced concepts such as the SpaceLiner cryogenic point-to-point transportation concept outlined in *ref. 3*. As part of the ongoing development activities, PMP is being reviewed and extended for the more accurate sizing of increasingly complex systems, such as propellant cross-feed systems and regulated ullage pressurisation. Validation and improvement of the models and sizing methods used within the program will be conducted in the course of these activities. The current work outlines the use of the publicly-available data for the Saturn-V rocket for this purpose.

2. PMP Modelling Approach

PMP is used to estimate the preliminary design parameters of fuel tanks and propellant systems. The basic input data includes the propellant masses and types, reference tank geometry parameters such as dome heights and tank lengths, materials, as well as trajectory- and time-dependent data such as propellant mass flow, engine mixture ratio and acceleration. With this input PMP is capable of approximately calculating the wall thickness, the geometry and the mass of the tanks and the feed- and pressurisation lines. Following the generation and sizing of the geometry, PMP is also capable of simulating over a specified mission thermodynamic and fluid behaviours, including stratification, heat flow from structures fluids, and evaporation and heat flow over the fluid-vapour interface. Ullage pressure regulation is also simulated over the course of the specified mission, with simplified control logic enacted allowing the pressure to be maintained within dictated bandwidths through venting or the injection of pressurant gas into tank ullages. This data is calculated and given for the different geometry nodes at each time step. The calculation methods employed in the program are 1-dimensional, and involve integral consideration of control volumes. Currently, only ideal gas laws are considered, however real gas law implementation is foreseen. An overview of the program is provided in Figure 1.

The calculation of the pressurisation system mass and required pressurant gas mass is highly sensitive to the functional parameters of required ullage pressure, and the storage and injection temperatures of the pressurant gases. The required gas mass for the pressurisation of the propellant tanks increases with decreasing temperature of the injected pressurant gas. However, the storage of non-reactive pressurant gases at low temperatures has the potential to provide mass savings, as the volume or pressure of the storage vessels can be decreased, and subsequently the vessel mass.

To address both of these needs, heat exchangers are often used to heat the cold gas to an optimal temperature before entering the propellant tank.[4] PMP therefore allows the specification of different storage and injection temperatures of pressurant gases to enable the sizing of the storage vessels while ensuring that realistic ullage fluid thermodynamic phenomenon are modelled.

The outputs of the analysis are required tank volumes, tank lengths, mass estimations for tanks, lines, insulation, line residuals and pressurant gas masses. These values provide important inputs to stage sizing, however the functional performance of the system is also provided, with flags raised to indicate non-nominal behaviour; for example when the ullage pressures exceed those specified or when geysering in lines is anticipated. System operational parameters are also provided, including evolutions of all tank ullage pressures, temperatures, line hydrostatic pressures, pressure drops, stratification, flow velocities and mass flows.

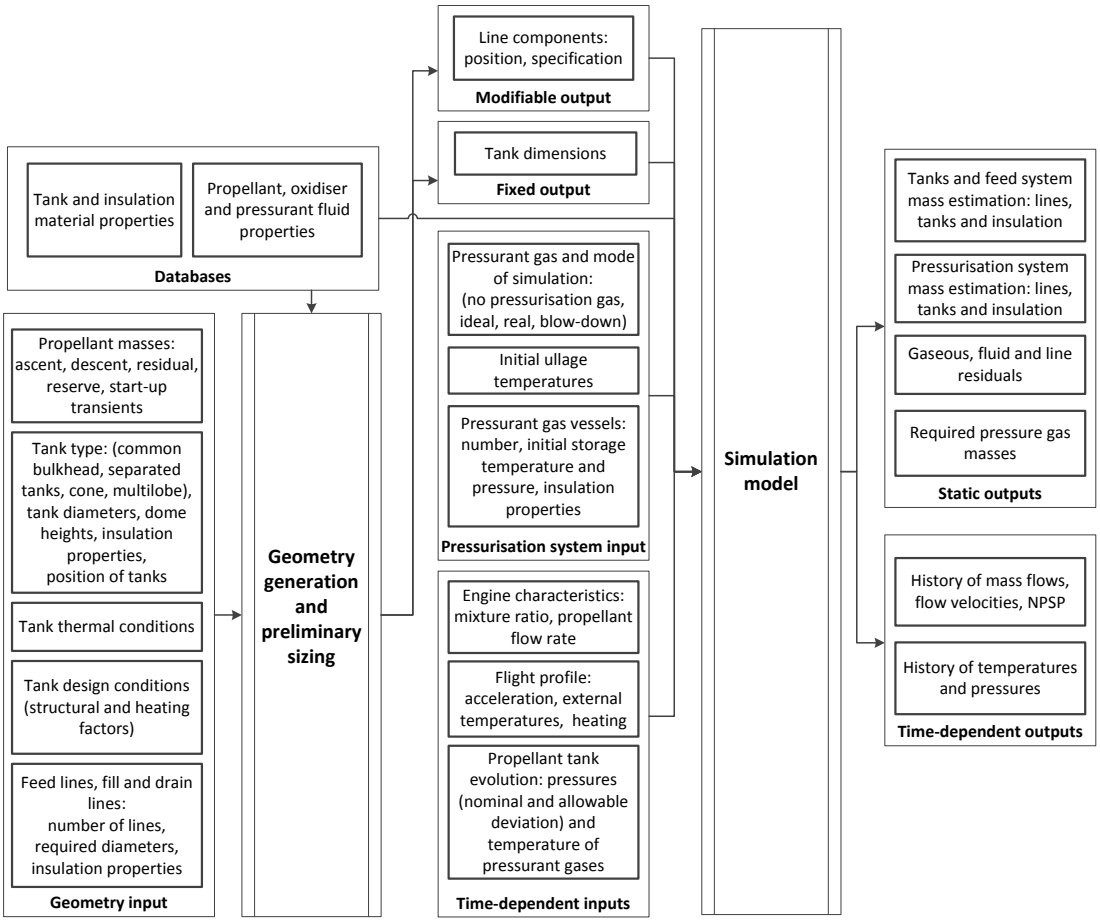

Figure 1: Overview of the inputs and outputs of PMP

3. Saturn-V Modelling

The Saturn-V was an American, human-rated expendable launch vehicle that was utilised in the National Aeronautics and Space Administration (NASA) Apollo and Skylab missions. The Saturn-V remains today the largest rocket ever launched, standing at 110.6 m tall and capable of bringing 118 tonnes to Low Earth Orbit (LEO) or 45 tonnes to Trans-Lunar Injection (TLI). A total of 15 vehicles were built, of which 13 flew. The AS-506 (Apollo 11 mission) was the sixth flight of the Saturn-V, and the fourth manned flight. Apollo 11 was launched at 09:32:00 (EDT) on July 16, 1969, from the Kennedy Space Center in Florida. The Saturn-V AS-506 successfully placed the manned CSM (command/service module) in a TLI coast and the Saturn-V Third Stage (S-IVB) and Instrument Unit (IU) were placed in a solar orbit with a period of 342 days. No serious anomalies or deviations occurred during the flight, and a wealth of flight and stage data has been released by NASA for public use. Input data for the simulation was sourced from flight data (*refs. 6, 7*) and stage fact sheets (*refs. 8–10*). [7]

The expendable AS-506 vehicle was composed of three liquid stages; the S-IC first stage using Kerosene (RP-1) and Liquid Oxygen (LO_2); and the S-II second stage and S-IVB third stage both using LH_2 fuel and LO_2 oxidiser. The staging was driven by the upper stages which are carried by other stages while fully loaded, and hence have a larger influence on the overall performance. The higher-specific impulse of LH_2/LO_2 countered its low-propellant density for these cases. The first and largest stage was designed to be compact while providing a moderate specific impulse, to avoid high atmospheric drag during the early ascent phases.[11] Information concerning these stages relevant to the performed simulations is outlined in further detail in this chapter. An overview of major flight events is provided in Table 1, with an overview of the principle dimensions provided in Table 2 and Figure 2.

Table 1: AS-506 major mission event summary[7]

Time Base	**Time [seconds]**	**Phase**
T0	−17.0	Guidance reference release
	−8.9	Saturn-V First Stage (S-IC) engine start sequence
	−6.4	S-IC engine start
T1	0.6	Umbilical disconnect
	66.3	Mach 1
	83.0	Maximum dynamic pressure
T2	135.3	S-IC CECO
T3	161.7	S-IC OECO
	460.6	Saturn-V Second Stage (S-II) CECO
T4	548.2	S-II OECO
T5	699.6	S-IVB ECO
T6	9278.2	Restart equation solution
	9320.2	S-IVB re-pressurisation
	9856.2	S-IVB re-ignition
T7	10203.3	S-IVB ECO

The vertical first stage was powered by a cluster of five F-1 engines. The LO_2 feedlines and conditioning lines ran directly through the RP-1 tank. The centre line was positioned vertically, and the four other lines radiated outwards from the top of the RP-1 tank to the base. Aluminium alloy 2219 was the predominant structural material.[11] Approximate dimensions are shown in Figure 2 (left).

The S-IC engines were ignited in the sequence centre engine; two opposing outer engines; and then the final two outer opposing engines.The F-1 engine flow rate and mixture ratio was time dependant; involving the Centre Engine Cut-Off (CECO) at a non-insignificant time prior to the Outer Engine Cut-Off (OECO). The mass flow rates and mixture ratios were averaged so that the five F-1 engines could use the same input file, with the mass flow rate set at 2647 kg/s and the mixture ratio at approximately 2.3 until CECO. The RP-1 tank was pressurised by Gaseous Helium (GHe) during the flight. This Helium was stored in four 3.51 m^3 vessels contained within the LO_2 tank. These vessels were pressurised to 21.37 MPa with a temperature of approximately 90 K. During the S-IC flight, this cold Helium was fed through F-1 engine heat exchangers before being fed to the RP-1 ullage. The LO_2 tank was pressurised during the flight with Gaseous Oxygen (GO_2) tapped off from the engine before entering the combustion chamber. Ullage pressure was maintained at 0.12 - 0.16 MPa, with a GO_2 flow rate of around 18 kg/s.[7,8]

The LO_2/LH_2 S-II second stage burned for approximately 6 minutes, with each of its five J-2 engines consuming propellant at a rate of approximately 247 kg/s with a mixture ratio of 5.5. The vertical stage has a common bulkhead configuration, with the upper LH_2 tank separated from the lower LO_2 by an aluminium-phenolic honeycomb sandwich. An overview of the stage is shown in Figure 2 (centre). The propellant tanks were pressurised by engine tap-off, with the LO_2 and LH_2 tanks being pressurised by GO_2 and Gaseous Hydrogen (GH_2), respectively. The pressure in the tanks was not actively controlled during the S-IC flight phase, up to 162 seconds into the flight. During the S-II-powered flight phases up to the S-II CECO, the LO_2 tank pressure was regulated to be between 0.248 - 0.265 MPa, and the LH_2 to be between 0.197 - 0.207 MPa. Following CECO, the operational ullage pressure window in the LH_2 tank was increased to 0.21 - 0.23 MPa.[7,9]

The LO_2/LH_2 S-IVB third stage used a single J-2 engine to supply approximately 1000 kN of thrust, burning the liquid propellants at a rate of approximately 215 kg/s with a mixture ratio of 5.0 during two boosts. The stage features a single tank, with the fuel and oxidiser separated by a common bulkhead. The stage geometry is depicted in Figure 2 (right). The cryogenic fuel and oxidiser tanks of the S-IVB stage were pressurised by different systems throughout the mission. The LH_2 tank pressure was not actively managed for the S-IC and S-II flight phases; however the LO_2 tank pressure was managed by Helium. The Helium was stored in cooled (27 K), pressurised vessels submerged in the LH_2 tank and during the early flight phases before J-2 engine operation, it was also injected into the LO_2 ullage

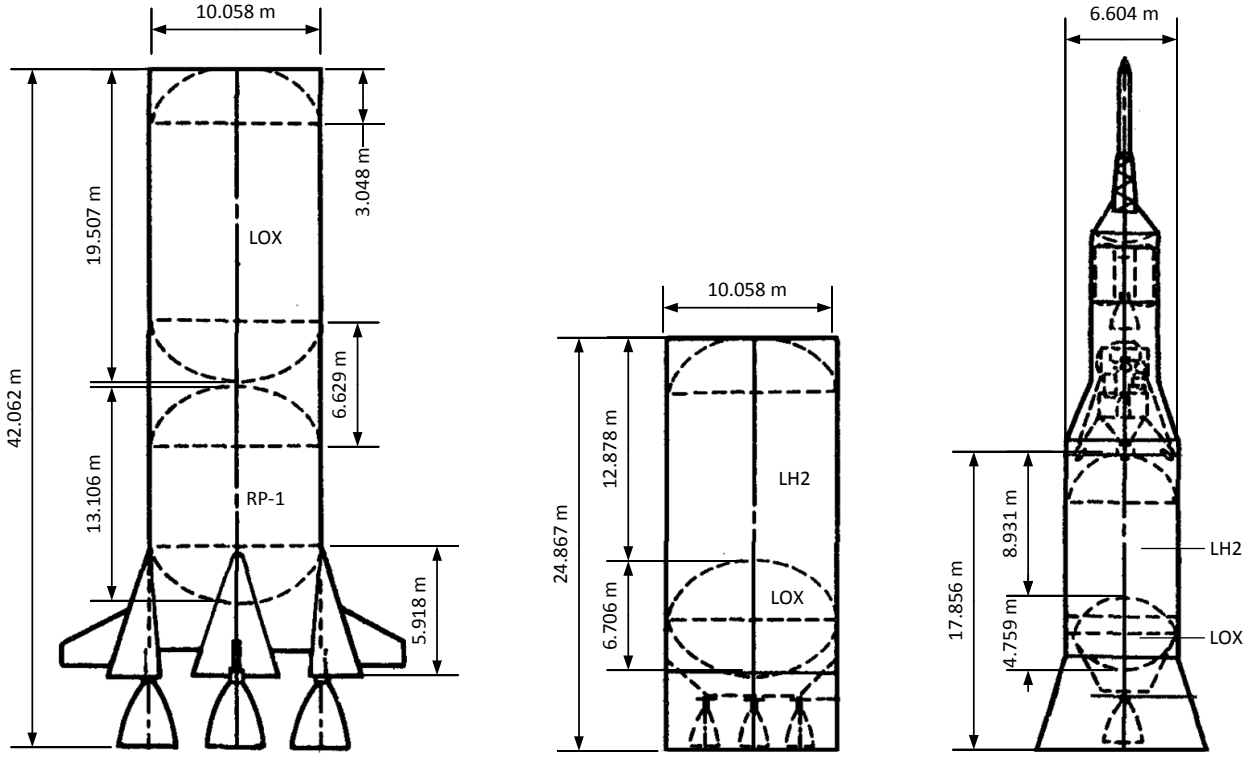

Figure 2: S-IC (left), S-II (centre) and S-IVB (left) dimensions[8–10]

unheated. During engine operation, the LH_2 tank was pressurised using GH_2 tapped from the engine, and the LO_2 tank was pressurised using heated Helium. The cold Helium was heated using an engine heat exchanger, and then recombined with a fraction of unheated Helium before being dispersed in the LO_2 ullage. During the long coasting phase in the parking orbit, the S-IVB stage was subject to fluctuating heat loads, and the unmanaged ullage pressures decayed significantly. Helium was then used for the re-pressurisation of both the LH_2 and LO_2 tanks before the second boost. Cold Helium heated using an GO_2-GH_2 burner was used for this pressurisation. A redundant system of ambient Helium vessels stored on the thrust frame was included for use in the event of the GO_2-GH_2 failure; however the operation of this system was not addressed in the frame of this work. The propellant tanks were pressurised during the second boost phase as per the first boost phase.[7,10]

As the type of pressurant gas could not be altered throughout the PMP simulation, three separate pressurisation models were used consecutively to model the complete third stage. The first of these models covered the ascent phase and the S-IVB first boost. The second model resumed at 699.6 seconds, and simulated the parking orbit flight and re-pressurisation with heated Helium gas. The final model simulated the second boost. These models are outlined in Table 3. Estimates for the Helium injection temperatures are also provided. Helium temperatures were not provided in the found literature, and therefore these assumptions were made based on experience, with the exit temperatures of eat exchanges roughly optimised through parameter studies.

Table 2: Principle dimensions of the Saturn V [8–10]

Parameter	Unit	S-IC	S-II	S-IVB
Stage				
Number of engines	-	5	5	1
Tank mixture ratio	-	2.302	5.177	4.419
Stage dry mass	kg	137 438	43 091	15 240
Ascent propellant	kg	20 844 429	439 005	103 614
Residual propellant	kg	31 995	3338	3458
Stage heat flux reduction factor[a]	-	0.15	0.15	0.3
Fuel tank radius	m	5.0292	5.0292	3.302
Fuel tank front dome height	m	3.048	3.048	2.353
Fuel tank aft dome height	m	3.048	-	-
LO_2 tank radius	m	5.0292	5.0292	3.302
LO_2 front dome height	m	3.048	3.048	2.353
LO_2 aft dome height	m	3.048	3.048	2.353
Feedlines				
Number of fuel feedlines	-	10	5	1
Fuel feedline diameter	m	0.4	0.2032	0.09[a]
Number of LO_2 feedlines	-	5	5	5
LO_2 feedline diameter	m	0.4	0.2032	0.09[b]
Fill and Drain (FD) lines				
Number of fuel FD lines	-	1	1	1
Fuel line maximum volume flow rate	m^3/s	0.13	0.63	0.63
Fuel FD line diameter	m	0.1524	0.2032	0.2032
Number of LO_2 FD lines	-	3	1	1
LO_2 FD line maximum volume flow rate	m^3/s	0.6309	0.79	0.79
LO_2 FD line diameter	m	0.1524	0.2032	0.2032
Pressurisation System				
Fuel pressurisation line diameter	m	-	0.05	0.05
Fuel pressurisation gas	-	GHe	GH_2	GHe/GH_2
Number of fuel press. gas tanks	-	-	N/A	5
Fuel pressurisation gas storage initial pressure	MPa	-	N/A	21
Fuel pressurisation gas storage initial temperature	K	-	N/A	27
LO_2 pressurisation line diameter	m	0.3	0.175	0.075
LO_2 pressurisation gas	-	GO_2	GHe	GHe
Number of LO_2 press. gas tanks	-	N/A	N/A	2
LO_2 pressurisation gas storage initial pressure	MPa	N/A	N/A	21
LO_2 pressurisation gas storage initial temperature	K	N/A	N/A	27

[a] Estimate, outlined in Chapter 4
[b] Estimate

Table 3: S-IVB sequential pressurisation models[7,10]

Model	Time [seconds]	Phase	LO_2 pressurisation	LH_2 pressurisation
1	0 - 552.2	S-IC and S-II flight phases	GHe 27 K 0.26 - 0.28 MPa	None
	552.2 - 699.6	S-IVB first flight phase	GHe 240 K 0.26 - 0.28 MPa	GH_2 110 K 0.21 - 0.23 MPa
2	699.6 - 9326.3	Parking orbit phase	None	None
	9320.2 - 9856.2	S-IVB re-pressurisation	GHe 290 K 0.26 - 0.28 MPa	GHe 290 K 0.21 - 0.23 MPa
3	9856.2 - 10203.3	S-IVB second flight phase	GHe 240 K 0.26 - 0.28 MPa	GH_2 110 K 0.21 - 0.23 MPa

4. Environmental Conditions and Stage Transient Inputs for the Saturn-V Analysis

The history input file of PMP allows for transient inputs to enable the simulation of the stage propellant behaviour over a complete mission.. This chapter outlines the generation of inputs for the simulated history evolution. These include the load in the x- and z-directions, aeroheating loads and environmental conditions including temperature and radiative heat flux. The x-axis loads until parking orbit insertion were taken from the AS-506 acceleration profile shown in Figure 3, with the environmental temperature for the stage determined from the altitude given in the ascent trajectory profile provided in *ref. 7* cross-referenced with the U.S. Standard Atmospheric Model.[12] This is shown in the graph to the left of Figure 4.

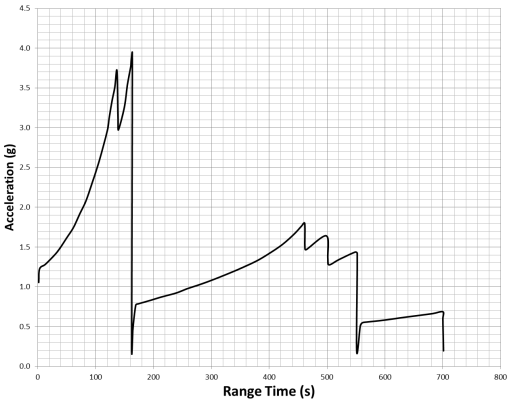

Figure 3: AS-506 Ascent trajectory acceleration (measured)[7]

The convective heat flux is the heat imparted to the tank external wall by the aerodynamic forces during the flight. No convective heat data for any stage was provided for the Apollo 11 mission; therefore flight data from the Apollo 4 AS-501 mission (*ref. 6*) was taken and adapted to the slightly-modified Apollo 11 flight profile. The evolution of the heat flux with respect to mission time was provided by sensor measurements located on the S-II fairing for the AS-501 mission. Measurements were also provided for the heat flux in the vicinity of the thrust bay for all stages; however the selected data was considered more representative as it was not strongly influenced by engine heat flux.[6] The S-II fairing sensor data was assumed for all stages, and extrapolated for S-IVB flight.

In typical practice during design activities, PMP obtains the convective heat flux from the DLR-SART trajectory simulation and optimisation program (TOSCA) output file. The heat flux is calculated in TOSCA using the following approximation:

$$\dot{q}_{convective} = C\sqrt{\frac{\rho R_{n,r}}{\rho_r R_n}}\left(\frac{v}{v_r}\right)^{3.05} \tag{1}$$

Where the correlation constant $C = 20254.4$ W/cm^2; ρ is the air density at the time-specific altitude; $\rho_r = 1.225$ kg/m^3 is the reference air density at sea level[12]; $r_r = 1$ m is the reference nose radius; $r_r = 0.914$ m is the launch vehicle fairing nose radius (estimated from LES cover); v is the vehicle velocity at the given time point (m/s) and $v_r = 10000$ m/s is the reference vehicle velocity. The heat flux model is shown in Figure 4, with a comparison to the adapted AS-501 flight data.

The heat flux generated from the flight data was found to have a much higher maximum value; however it also increased and declined at a steeper rate than the heat flux model. The flight data was taken as the input for PMP. This is, however, close to the maximum heat flux, that is, the heat flux at the stagnation point and therefore this value must be scaled to determine the heat flux at the tank bays. The scaling factor is provided in the PMP input file, and the values of these are provided in Table 2.

The radiative heat flux was modelled for two cases; the hot case, where solar and albedo fluxes were considered; and the cold case, where the solar and albedo fluxes were discounted, and the Earth Infrared (IR) was selected to be a minimum value. These two cases were chosen to represent when the spacecraft was in sunlight (case 1) or in the shade, as would occur during the eclipse of the sun by the Earth in the parking orbit (case 2). To account for the variation with altitude, the heat flux (in W/m^2) was determined for each case by scaling with air density:

$$\dot{q}_{rad} = \dot{q}_{rad,max} - \left(\dot{q}_{rad,max} - \dot{q}_{rad,min}\right)\frac{\rho}{\rho_0} \tag{2}$$

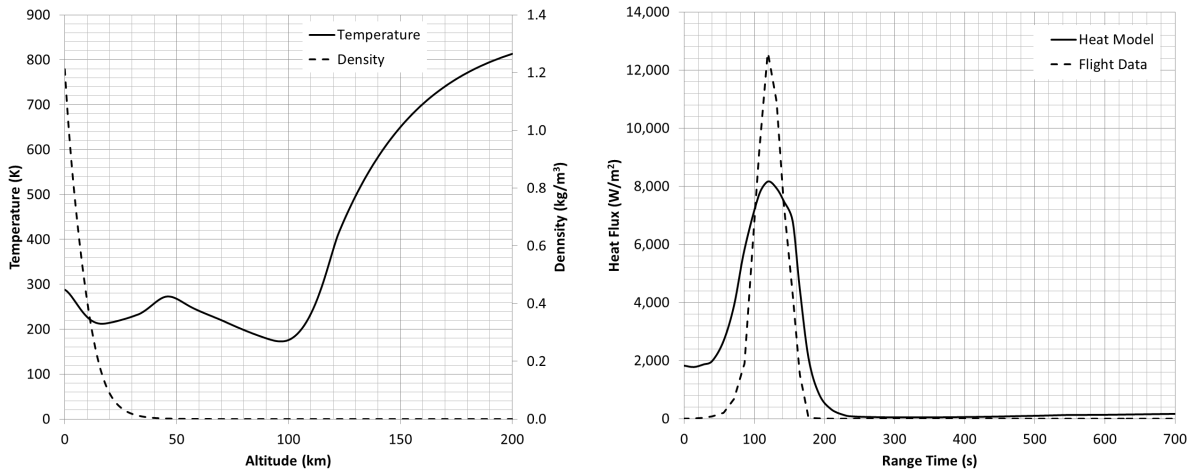

Figure 4: Atmoshperic model (left) and ascent phase convective heat flux (right)

Where ρ is the air density at the given altitude (kg/m^3), ρ_0 = 1.173 kg/m^3 is the reference density, $\dot{q}_{rad,min}$ = 500 W/m^2 and $\dot{q}_{rad,max}$ is the maximum heat flux (W/m^2), given by:

$$\dot{q}_{rad,max} = \dot{q}_{rad,solar} + f_{albedo} \cdot \dot{q}_{rad,solar} + \dot{q}_{rad,IR} \tag{3}$$

$\dot{q}_{rad,solar}$ is the solar constant, 1367 W/m^2 for the hot case, and 0 W/m^2 for the cold case; f_{albedo} is the fraction of solar radiation reflected by the Earth, taken to be 0.57 for the given orbital parameters; and $\dot{q}_{rad,IR}$ is the Earth's infrared heat flux. For the given orbital inclination of 32.521° and period of 88.18 minutes,[7] this was selected to be 257 W/m^2 for the hot case, and 218 W/m^2 for the cold case.[13]

In order to determine the period of the eclipse, the orbit beta angle β was determined. This is the minimum angle between the orbit plane and the solar vector, for the launch date July 16 1969 and Eastern Daylight Time (EDT) 9:32:00,[7] it was found that $\beta = 23.9^o$ and resulting in a fraction of 0.488 of the 88.18-minute orbit being in shadow. The starting time of the eclipse was approximated to be 2000 seconds from the start of the mission from temperature measurements shown in *ref. 7*. The radiative heat environment derived from the calculated eclipse period phases and mission sequences are shown in Table 4.[14]

Table 4: Radiative heat environment

Time [seconds]	**Phase**	$\dot{q}_{rad,min}$	$\dot{q}_{rad,max}$
0 - 2000	Ascent / parking orbit, sun	500[a]	2403
2000 - 4585	Parking orbit, eclipse	-	218
4585 - 7293	Parking orbit, sun	-	2403
7293 - 9878	Parking orbit / S-IVB second burn, eclipse	-	218
9878 - 10213	S-IVB second burn, sun, constant	-	2403

[a] Varied using Equation 2

5. Preliminary Sizing Results

This chapter outlines the preliminary sizing results; namely the tank dimensions including lengths and wall thickness, and the subsequent tank and line masses.

The propellant mass, and therefore propellant tank volumes, is one of most important factors in the iterative, preliminary design process of launch vehicles. As such, the propellant mass values evolve throughout the design definition, and this has driven the need for the quick resizing of the propellant tanks under the constraints of previous design decisions. A change in volume of the tanks can be accommodated by either changing the tank diameter, dome height or tank length. Typically, tank length is the parameter that is subsequently varied as it has a minimal impact on the design before the structural analysis phase of the design process, and the factors of diameter and dome height are constrained by existing operational parameters such as existing tooling and infrastructures. To accommodate this practice in normal design activities, tank lengths are not specified as the input for PMP; with the propellant mass, storage conditions and tank factors are used to size the tanks with diameter and dome height constrained. Additional tank factors; namely the

the ullage factor which states which fraction between the gaseous ullage and the liquid propellant at the beginning of the simulation; and the tank structure factor, which defines the fraction of the tank internal volume that is occupied by structural elements; are also applied. Therefore, in the AS-506 model, the ullage and structural factors were varied until the specified length dimensions were achieved. The selected factors and the corresponding sized tank lengths are shown in Table 5. The resulting geometric models of the three AS-506 stages are shown in Figure 5. The resulting ullage factors are typical for the respective stage types[4]

Table 5: Sizing factors for the Saturn-V propellant tanks

Parameter	Unit	S-IC	S-II	S-IVB
Dimensions				
Fuel tank height[8–10]	m	13.1	12.9	8.9
LO_2 tank height[8–10]	m	19.5	6.7	4.8
Factors				
Fuel tank ullage factor	-	0.97	0.97	0.97
Fuel tank internal structure reduction factor	-	0.95	0.98	0.98
LOX tank ullage factor	-	0.99	0.98	0.98
LOX tank internal structure reduction factor	-	0.95	0.98	0.98

The tank wall thickness and subsequently the masses were then calculated by PMP. The results are shown in Table 6, with a comparison to data found in *ref. 11*. A comprehensive mass breakdown of the Saturn-V rocket series is not available publicly, however this reference publication condenses data from a Apollo 16 AS-511 operational mass characteristics report.

Table 6: Saturn-V mass estimation

Parameter	Unit	Value PMP	Reference[11]	Discrepancy
S-IC				
Tank mass[a]	kg	11350	25873	-56.1%
Plumbing mass	kg	3142	16100	-80.5%
S-II				
Tank mass	kg	10346	12680	-18.4%
Plumbing mass	kg	801	3480	-77.0%
S-IVB				
Tank mass	kg	3279	3947	-16.9%
Plumbing mass	kg	379	1530	-75.2%

[a] Includes wall insulation mass

It was generally found that the mass estimations for the structural elements were significantly lower than the actual values. PMP considers the internal ullage pressure and the pressure exerted by the fluid mass, tapering the tank from the bottom to the top to account for this. The specified stage accelerations are also considered, however these static loads are not generally the sizing loads for large stages, for which dynamic launch pad, gust or guidance and control system-driven stiffness requirements tend to be the critical loads.

It can be seen in Table 6 that the error in the estimated values decreases for the second and third stages. Considering the staging and flight loads, this is consistent with expectations. The overall trend from the reference mass data is toward reduced structural mass higher in the vehicle due to decreasing loads. The five F-1 engines act on the S-IC first stage with a force per unit area exceeding the tank pressures.[11] Furthermore, at the end of the first stage burn, 80% of the remaining vehicle mass is located above the empty first stage, requiring the thrust to be transmitted through the entire empty stage to the S-II LO_2 tank, where the largest fraction of the stage mass at this time point is centred. As such, the pressurisation of the S-IC tanks is performed for stabilisation against buckling, in addition to the engine feed requirements, and these tanks have additional structural stiffening.[11]

The tank skins are far more than simple shell structures. The tanks skins have integral stiffeners, while skirt, interstage and intertank structures not subject to internal pressure loads were allowed to deviate from cylindrical shells, incorporating corrugation to increase stiffness and to avoid buckling.[8,11] Additionally, the commonbulkeads and tank domes are modelled with a constant thickness in PMP, however in reality the thickness tapers away toward the outer edge, as the aluminium structure must be continuous at the outer shell to carry axial loads.[9] The equivalent cylindrical shell thickness and the corresponding thickness calculated by PMP are given in Table 7. In this table it can also be seen that the equivalent thickness of the tanks increases significantly for the lower stages.

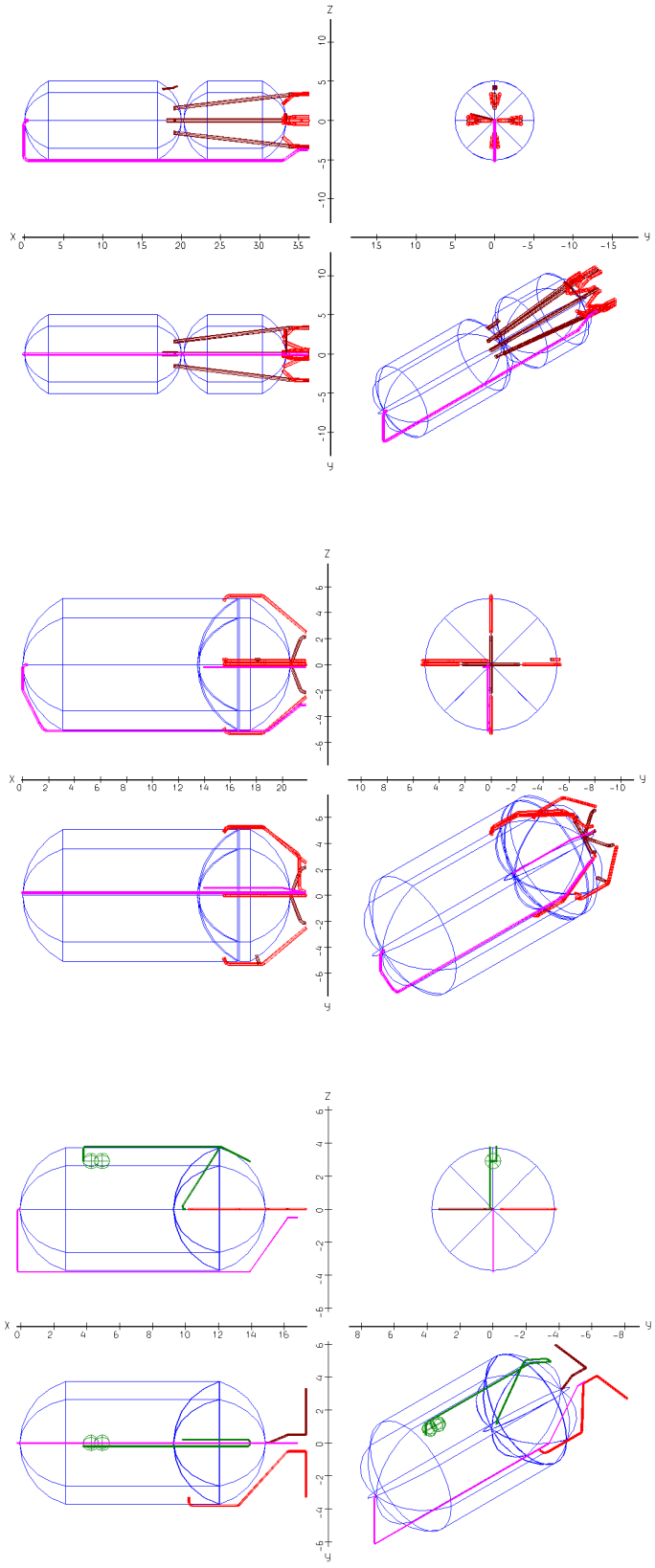

Figure 5: S-IC (top), S-II (center) and S-IVB (bottom) stages modelled in PMP. Note; the GHe storage vessels for the pressurisation of the S-IC RP-1 tank are absent; and the GHe vessels for the S-IVB LO_2 tank management only are shown

Table 7: AS-506 tank thickness (shell equivalent)

Parameter	Unit	Value PMP	Reference[11]	Discrepancy
S-IC				
Maximum LO_2 tank thickness (bottom)	mm	4.6	6.6	-30.2%
Minimum LO_2 tank thickness (top)	mm	1.8	4.9	-63.6%
Maximum fuel tank thickness (bottom)	mm	3.0	4.9	-38.1%
Minimum fuel tank thickness (top)	mm	1.9	4.3	-55.7%
S-II				
LO_2 tank thickness (top)	mm	2.3	4.7	-50.4%
Common bulkhead thickness	mm	2.5	4.7	-45.8%
Fuel tank thickness (bottom)	mm	5.0	4.7	+6.2%
S-IVB				
LO_2 tank thickness (bottom)	mm	2.2	3.4	-34.0%
Common bulkhead thickness	mm	1.4	3.4	-60.1%
Fuel tank thickness (cylinder)	mm	1.8	3.4	-47.3%

The discrepancies in plumbing (line) masses can be attributed to line stiffeners, attachments and insulation masses. The most prominent examples of these discrepancies are the unsupported LO_2 feedlines in the S-IC stage, which are themselves 0.43 m in diameter diameter ducts run inside 0.64 m tunnels installed through the fuel tank, contributing a large fraction (11.5 tonnes) to the S-IC plumbing mass; and the fuel and oxidiser lines in the S-II and S-IVB stages, which are vacuum-jacketed.[11]

6. Simulation and Ullage Evolution Results

The simulation of the tank ullage, fluid and line evolutions presented several challenges, including replication of complex pressurisation systems, however it also revealed the strong interdependence between tank insulation masses and pressurant gas masses and highlighted the need to be able to perform parametric optimisation to find the lightest mass solution. This chapter outlines key results, including ullage pressure and temperature evolutions and pressurant gas masses. An overview of the latter is provided in Table 8.

Table 8: Saturn-V pressurant gas mass estimations

Parameter	Unit	Value PMP	Reference[11]	Discrepancy
S-IC				
GO_2 for pressurisation	kg	3432	3400	+0.9%
GHe for pressurisation	kg	-	240	-
S-II				
GO_2 for pressurisation	kg	2896	1900	+52.4%
GH_2 for pressurisation	kg	492	-	-
S-IVB				
GO_2 for pressurisation	kg	24	-	-
GHe for pressurisation	kg	181	171	+5.8%
GH_2 for pressurisation	kg	88	-	-

The S-IC simulation was found to be comparable to the flight data, with the exception of the RP-1 pressurisation system which could not be simulated. The flight ullage pressure and relief value limits and consumed GO_2 are shown in Figure 6 (left). While the ullage pressure remains consistent to the reference value provided in *ref. 8*, it does not match the flight data from *ref. 7*, which, while staying within the set limits, deviated from the reference value, particularly near the end of the S-IC flight phase. One explanation for this is the LO_2 tank pressure control system. The control logic for the ullage pressure control system is not provided in any reference, however from consideration of the mission events provided in the literature, it is likely that the control system on the real S-IC stage was open; that is, the valves were controlled to follow a pre-programmed sequence rather than receiving feedback from ullage pressure sensors, which cannot be simulated in PMP.

The GO_2 delivery temperature was then varied until it fit with the reference data, resulting in an increase from 100 K to 180 K, where it showed good correspondence to the flight data. The corresponding ullage temperature evolution is shown to the right of Figure 6. A compromise had to be made, as no value for the delivery temperature could be

found that satisfied both the flow rate and total mass conditions. Therefore, the simulated consumed GO_2 (provided in Figure 6 and Table 8) was slightly higher than the provided reference value.

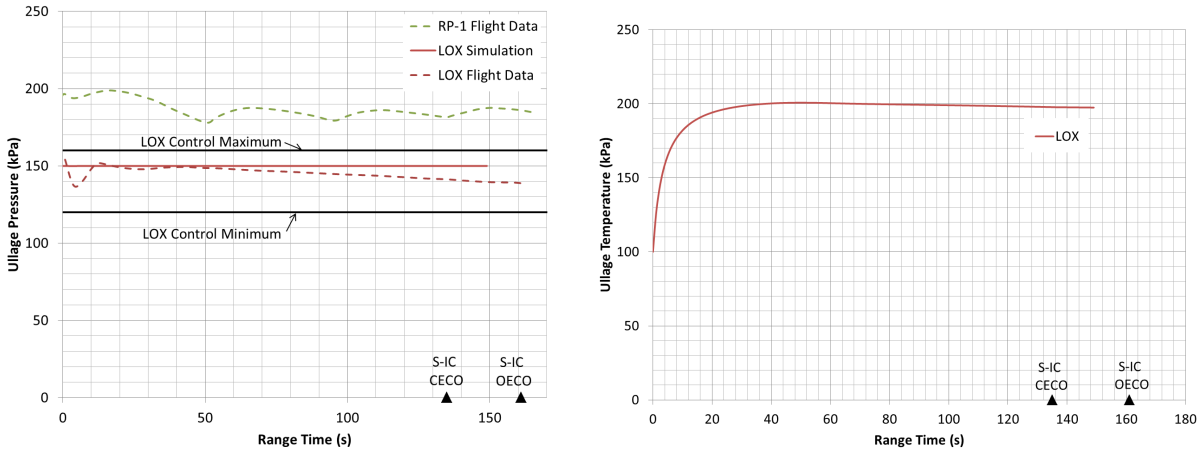

Figure 6: S-IC LO_2 ullage pressure evolution and GO_2 pressurant gas mass flow rate (left), and S-IC LO_2 ullage temperature evolution (right). Flight data from *ref. 7*

Following the initial modelling of the S-II stage, it was found that extremely high ullage pressures, reaching maximum of around 0.5 MPa were present in both tanks, corresponding to the peak in convective heat flux shown in Figure 4 (right). Considering the flight data for the stage (displayed as the dashed line in the graph to the left of Figure 7), these values were considered excessive. Assessed causes were excessive environmental temperature; inadequate stage insulation and the need for venting during the S-IC flight phase. Therefore, a venting control system was added. The venting capabilities of PMP are limited; with the use specifying only the maximum upper and lower deviation from the reference value; the venting valve number and diameter; and the response time. Advanced control logic is not implemented, with valves being in either completely open or closed states. Two venting valves were used per tank (from *ref. 9*), with response times of 1 second and diameters of 11 mm and 18 mm for the LO_2 and LH_2 tanks, respectively. These values were selected after several iterations. The resulting, fitted ullage pressure evolutions are shown in Figure 7 (left) with the corresponding temperature evolutions shown to the left. The implementation of the venting system did, however result in a larger pressurant gas requirement, with PMP utilising approximately 50% more GO_2 than the flight data indicates (see Table 8).

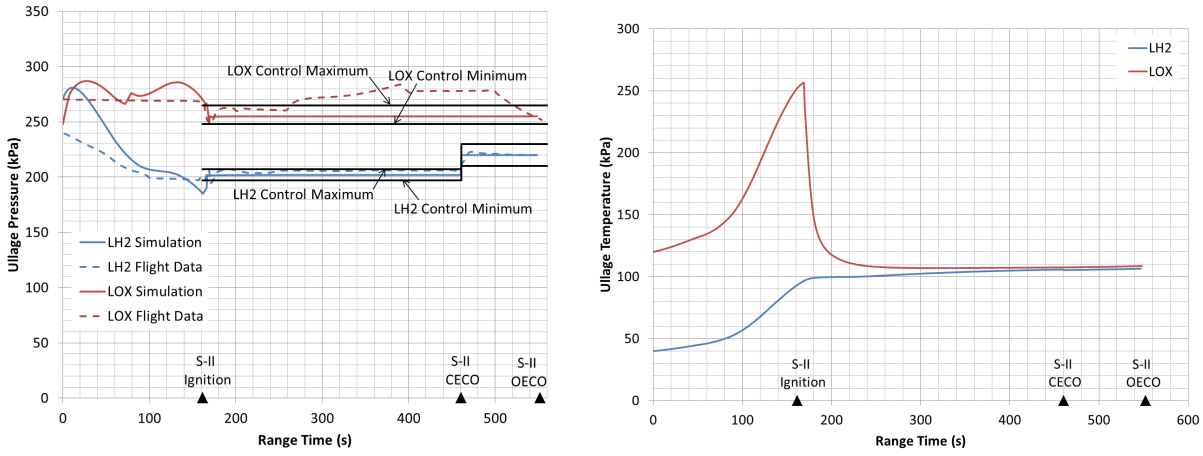

Figure 7: S-II ullage pressure evolutions (left), and S-II ullage temperature evolutions (right). Flight data from *ref. 7*

Due to the various pressurisation phases, long mission duration, limited information concerning the tank venting and the complex external environment, the S-IVB was the hardest stage to model. The simulation results for this stage are displayed in Figure 8, which an overview of the performance for the entire mission duration (consolidation of all models outlined in Table 3).

During the long coasting phase, the propellant tanks were vented at the discretion of the ground command.

Significant event data, including venting, was provided in *ref. 7*; however this method of venting could not be simulated due to the simplicity of the PMP venting model. Furthermore, the valve diameters were not provided. The valve diameters and response times were sized based on the critical coasting phase. Two venting valves were used for the LO_2 tank, with a response time of 10 seconds and a diameter of 3.5 mm. Three valves with diameters of 5.3 mm and a response time of 10 seconds were used for the venting of the LH_2 tank. These values were selected after several iterations, however a suitable solution was difficult to achieve in either case as either the system showed excessive oscillation due to an overly high vent value diameter or unsuitable response time; the pressure remained too high due to insufficient valve diameter; or there was a calculation error in the code; caused by excessive venting. It can be seen in Figure 8 (left) that a high level of fluctuation is evident in the solution implemented for the LO_2 tank, and that an insufficient valve diameter must be used for the LH_2 solution.

The temperature evolution of the stage using an insulation thickness of 60 mm is shown to the right of Figure 8. For this insulation thickness, the vented ullage gas mass was found to be 348 kg, and the LO_2 and LH_2 boil off masses were found to be 106 kg and 359 kg, respectively. In comparison to data provided in *ref. 11*, the LO_2 boil off is remarkably high (reference data quoting 24 kg) and the LH_2 value is significantly lower than the 1 tonne specified. This can be attributed to several causes, including uncertainties in the heat flux values, insulation properties and the pressurant gas injection temperatures. Considering the opposing trends for the two tanks, it is likely that the latter is the most significant contributor, in addition to lower commonbulkhead heat transfer in the simulation.

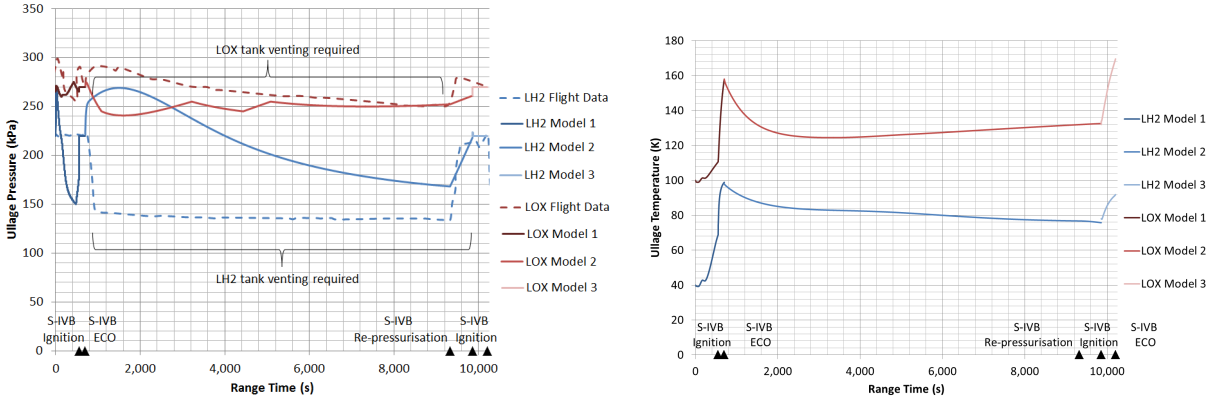

Figure 8: S-IVB LO_2 ullage pressure evolution and GO_2 pressurant gas mass flow rate (left), and S-IVB LO_2 ullage temperature evolution (right). Flight data from *ref. 7*

The effectiveness of the herein described pressurisation schemes were then assessed through examination of the engine NPSPs throughout the mission. The minimum pressure at the outlet of the feedlines throughout the periods of engine operation was found for all stages, and compared to the reference minimum value required by the engines for nominal operation. The simulated feedline NPSP was found to be satisfactory for all engines and all stages with the exception of the S-IVB LO_2 feedline, which exhibited a pressure slightly below the required. This can be attributed to excessive line losses created by geometric uncertainties in addition to the fluctuation of the LO_2 ullage pressure. Note that the minimum NPSPs for engine operation were taken from digitisation of graphical data from the AS-501 flight, and therefore have a high uncertainty (approximately ±10%) and may indeed be different for the AS-506 flight.

Table 9: Saturn-V engine NPSP comparison

Parameter	Unit	Value PMP	Minimum Allowable[6]	Discrepancy
S-IC				
LO_2 turbopump minimum NPSP	MPa	0.57	0.56	+0.010
Fuel turbopump minimum NPSP	MPa	-	0.29	-
S-II				
LO_2 turbopump minimum NPSP	MPa	0.134	0.129	+0.005
Fuel turbopump minimum NPSP	MPa	0.049	0.044	+0.005
S-IVB				
LO_2 turbopump minimum NPSP	MPa	0.139	0.143	-0.04
Fuel turbopump minimum NPSP	MPa	0.079	0.044	+0.035

7. Recommendations

In the quest to reduce stage inertial masses, future developments in the launch vehicle industry could involve solutions where the gaseous propellants themselves are used for pressurisation, similar to the method herein described for the Saturn-V rocket. The vaporised propellant is tapped off from the engine cycle and injected back into the tank. However, in the case of pressurisation of the upper stage, there are long periods either during the flights of the previous stages or during ballistic coasting phases, where the tank pressures must be regulated when the engine is not operating. This necessitates the use of a supplementary second system that employs a neutral pressurant gas such as Helium during these phases. It is therefore imperative to be able to model the combination of systems in the frame of preliminary pressurisation system design. The pressurisation system and pressurisation sequence of the Saturn-V rocket is highly complex, with more than one type of pressurant gas being used to the pressurise the same tank in some cases. To simulate the pressurisation of the tanks following this strategy, approximations in the PMP model had to be made. The method of using consecutive models was found to be inadequate; even if all characteristics from the last time point of the previous simulation are carried-over (temperature, pressure, ullage volume), the vapour mixture cannot be considered at all, significantly impacting the solution.

Through the comparison of the estimated pressurant gas masses and tank ullage pressure evolutions, it was found that PMP provides a reasonable output that is suitable for preliminary sizing purposes. However, simulation of regulation of tank pressure can be further refined to produce more true-to-life systems and aid parametric optimisation. The current model allows the specification of the permissible maximum upper and lower deviation from the reference tank pressure value; the venting valve number and diameter; and the valve response time. Advanced control logic is not implemented, with venting and inlet valves being either open or closed when exceeding or falling below these limits. This method can result in a pressure-profile such as that for the LH_2 shown in Figure 8 if values for the valve diameter are selected to restrict the flow. The alternative to this solution is a pressure-profile in which the pressure fluctuates between the minimum and maximum values, with venting used to reduce excessive pressures. Hence, the pressurant gas consumption was often found to be higher in the simulation due to excessive venting.

As herein described, the storage temperature and injection temperature of pressurant gases are both given by the program user. However the heating of the pressurant is not considered at all. Heaters, either in the form of additional GO_2-GH_2 heaters or engine heat exchangers, could add significant mass to the pressurisation system and negate the mass gains of cold storage. Furthermore, the heat flux between the propellant and Helium storage vessels should be modelled, to be able to accurately model the case of submersion of the latter in the cryogenic propellant.

Furthermore, it is recommended that the external temperature and heat flux models are refined, to enable a more accurate sizing of the pressurisation system masses. This encompasses the inclusion of an eclipse model, such as outlined in Chapter 4, and an engine heating model.

The program PMP can only address one stage at a time. Consequently, the time-dependent inputs must be generated for each stage individually. Heat transfer from other stages (not relevant for the Saturn-V rocket, however common to parallel-staged launchers) is therefore also not considered. Furthermore, while a simplistic sizing method using the maximum stage load is implemented, this does not account for the specific load cases as various tanks and bays, which evolve throughout the flight as preliminary stages are jettisoned and propellant is consumed. One notable case where it is imperative that this is considered is the first stage LO_2 tank, which experienced very high compressive loads at the end of the first stage burn. Consequently, the mass and skin thickness estimations for the stage were too low. However, upper stage tanks which are not subject to such extreme cases saw more accurate mass predictions. To address these global structural assessment needs and allow for holistic heating considerations while simplifying model generation, it is therefore recommended that the stage tanks should be able to be modelled in one simulation, with additional sizing methods such as the beam method employed for sizing of tanks skin thickness.

8. Conclusion

In conclusion, the modelling of the Saturn-V stages' propellant storage, feed and pressurisation system was successfully performed despite the high system complexity. While the functional operation of the modelled propellant systems were highly consistent with reference flight data, the preliminary mass estimates for lines and tanks were found to be significantly below provided values. An investigation into the structural sizing cases of the Saturn-V rocket revealed that, particularly in the case for the lower stages, the methods employed by PMP were insufficient.

PMP was found to be an effective tool for the simulation of the fluid and thermodynamic phenomenon, however for it to be employed as an effective design tool, the tank sizing methodology and pressurisation system implementation need to be adapted and further developed. Without these improvements, the tool can only be utilised by experienced engineers who are able to knowledgeably adapt the input parameters and select the most relevant and realistic program outputs and discard those which are invalid.

Acknowledgements

The authors would like to thank Carina Ludwig and Martin Sippel for contributing their knowledge to the application of the herein mentioned development tools.

References

[1] Ludwig, C. and Dreyer, M. (2012) Analyses of Cryogenic Propellant Tank Pressurization based upon Ground Experiments. *AIAA SPACE 2012 Conference & Exposition*.

[2] Letchworth, G. (2011) X-33 Reusable Launch Vehicle Demonstrator, Spaceport and Range. *AIAA SPACE 2011 Conference & Exposition*.

[3] Schwanekamp, T. (2014) Cryogenic Propellant Tank and Feedline Design Studies in the Framework of the CHATT Project. *19th AIAA International Space Planes and Hypersonic Systems and Technologies Conference*.

[4] Clark, V. (2012), Optimisation of the Helium Storage System of a Launch Vehicle Cryogenic Upper Stage.

[5] Sippel, M., Dumont, E., Clark, V., Koch, A., David, E., Garbers, N., Manfletti, C., Höck, B., and Geiss, G. (2014) Advanced Launcher Options under Constraints of Synergy, Commonality and Affordability. *65 th International Astronautical Congress*.

[6] National Aeronautics and Space Administration (1968), NASA-TM-X-60911 Saturn V Launch Vehicle Flight Evaluation Report: AS-501 Apollo 4 Mission.

[7] National Aeronautics and Space Administration (1969), NASA-TM-X-62558 Saturn V Launch Vehicle Flight Evaluation Report: AS-506 Apollo 11 Mission.

[8] National Aeronautics and Space Administration (1968), Saturn V News Reference First Stage Fact Sheet.

[9] National Aeronautics and Space Administration (1968), Saturn V News Reference Second Stage Fact Sheet.

[10] National Aeronautics and Space Administration (1968), Saturn V News Reference Third Stage Fact Sheet.

[11] Whitehead, J. (24 July 2000 - 28 July 2000) Mass breakdown of the Saturn V. *36th AIAA/ASME/SAE/ASEE Joint Propulsion Conference and Exhibit*.

[12] Minzner, R. A. (1977) The 1976 Standard Atmosphere and its relationship to earlier standards. *Reviews of Geophysics*, **15**, 375.

[13] Wertz, J. R. and Larson, W. J. (1999) *Space mission analysis and design*. Space technology library, Microcosm and Kluwer, 3rd ed edn.

[14] Gilmore, D. G. (ed.) (2002) *Spacecraft Thermal Control Handbook - Volume 1: Fundamental Technologies*.